Orig Life Evol Biosph (2013) 43:77–98
DOI 10.1007/s11084-013-9332-7

PREBIOTIC CHEMISTRY

Atmospheric Production of Glycolaldehyde Under Hazy Prebiotic Conditions

Chester E. Harman · James F. Kasting · Eric T. Wolf

Received: 20 February 2013 / Accepted: 11 April 2013 /
Published online: 22 May 2013

Abstract The early Earth's atmosphere, with extremely low levels of molecular oxygen and an appreciable abiotic flux of methane, could have been a source of organic compounds necessary for prebiotic chemistry. Here, we investigate the formation of a key RNA precursor, glycolaldehyde (2-hydroxyacetaldehyde, or GA) using a 1-dimensional photochemical model. Maximum atmospheric production of GA occurs when the CH_4:CO_2 ratio is close to 0.02. The total atmospheric production rate of GA remains small, only 1×10^7 mol yr^{-1}. Somewhat greater amounts of GA production, up to 2×10^8 mol yr^{-1}, could have been provided by the formose reaction or by direct delivery from space. Even with these additional production mechanisms, open ocean GA concentrations would have remained at or below $\sim$1 μM, much smaller than the 1–2 M concentrations required for prebiotic synthesis routes like those proposed by Powner et al. (Nature 459:239–242, 2009). Additional production or concentration mechanisms for GA, or alternative formation mechanisms for RNA, are needed, if this was indeed how life originated on the early Earth.

Keywords Prebiotic · Atmosphere · Chemistry · Glycolaldehyde · Fractal haze

Electronic supplementary material The online version of this article (doi:10.1007/s11084-013-9332-7) contains supplementary material, which is available to authorized users.

C. E. Harman (✉) · J. F. Kasting
Department of Geosciences, Penn State University, University Park, PA 16802, USA
e-mail: ceharmanjr@psu.edu

E. T. Wolf
Laboratory for Atmospheric and Space Physics, Space Science Building (SPSC), University of Colorado, 3665 Discovery Drive, Boulder, CO 80303-7820, USA

Introduction

The difficulty of forming RNA prebiotically has long been one of the greatest stumbling blocks for theories of the origin of life. Spark discharge experiments (simulating lightning) have been used to generate amino acids (Miller 1953; Cleaves et al. 2008), RNA precursor species like peptide nucleic acid (PNA) (Nelson et al. 2000), some nucleobases, in conjunction with eutectic freezing (Menor-Salván et al. 2009), and have been conjectured to form sugars (Schlesinger and Miller 1983), while forming ribose prebiotically is challenging (Shapiro 1984, 1988). Furthermore, hooking ribose together with pyrimidine nucleobases has long been considered difficult or impossible (Szostak 2009). Recently, Powner et al. (2009) discovered a way around this last problem by way of a novel multi-step ribonucleotide synthesis mechanism that bypasses the need for free sugars and nucleobases. As starting materials, their mechanism requires cyanamide (CN_2H_2), cyanoacetylene (C_3HN), glycoaldehyde ($HOCH_2CHO$), glyceraldehyde ($C_3H_6O_3$), and inorganic phosphate. These compounds could conceivably have been brought in by comets or asteroids (Chyba et al. 1989, 1990) or micrometeorites (Maurette et al. 2000), or they could have been formed in situ on the early Earth. Here, we estimate the rate of formation of these compounds on the early Earth, focusing in particular on the key compound glycoaldehyde.

The key to forming any of the first four compounds in the atmosphere is to have an environment in which methane can polymerize to form higher hydrocarbons. Both photochemical models (Haqq-Misra et al. 2008; Domagal-Goldman et al. 2011) and laboratory experiments (Trainer et al. 2006) predict that methane should polymerize if the CH_4:CO_2 ratio exceeds ~0.1. Our current model focuses on a lower ratio of 0.02, where peak production for GA and a modest amount of polymerization occurs. CO_2 levels in the early atmosphere are largely unconstrained, with various authors predicting either very high values (Walker 1985) or very low ones (Sleep and Zahnle 2001). Paleosols suggest that CO_2 concentrations were 10–50 times present (0.004–0.02 bar) at 2.7 Ga (Driese et al. 2011), but CO_2 concentrations prior to this time could have been much higher in order to keep the early Earth warm. CO_2 partial pressures exceeding ~0.03 bar produce enough greenhouse warming to resolve the faint young Sun problem, particularly when supplemented by CH_4 (Haqq-Misra et al. 2008). Other methods to solve the faint young Sun problem include alternative models for solar evolution (Gaidos et al. 2000), novel greenhouse gases such as ammonia (Sagan and Chyba 1997) and carbonyl sulfide (OCS) (Ueno et al. 2009), and changes in cloud type and surface albedo (Rosing et al. 2010); these arguments will not be tested in this work. Here, the model calculations are performed at a lower CO_2 partial pressure, 0.005 bar, to best remain in the regime of possible prebiotic methane concentrations and still explore a broad range of CH_4:CO_2 ratios (see the Model Description section for more details).

CH_4 should have been easy to come by in the biotic era if methanogens evolved early (Kharecha et al. 2005), but whether it would have been present in high concentrations in the prebiotic era is uncertain (Emmanuel and Ague 2007; Lazar et al. 2012; Fegley and Schaefer 2012). For a 1-bar N_2-dominated atmosphere, a CO_2 partial pressure of 0.005 bar, and a CH_4:CO_2 ratio of 0.02, the required volume mixing ratio of CH_4 to induce polymerization would be ~100 ppmv (~1×10^{-4} bar).

This is large but not implausible. (See further discussion below.) So, we will henceforth assume that a thin organic haze was present in the prebiotic atmosphere.

Glycoaldehyde is formed in today's atmosphere by oxidation of ethene (C_2H_4) and isoprene (C_5H_8) (Bacher et al. 2001; Magneron et al. 2005; Karunanandan et al. 2007). Ethene is a predicted gasous component of a hazy Archean atmosphere (Pavlov and Kasting 2001; Domagal-Goldman et al. 2011). Formation of glycoaldehyde from ethene is discussed in the next section. Glycoaldehyde can also be formed by way of the formose reaction, which involves polymerization of formaldehyde (H_2CO) in an aqueous solution (Butlerov 1861; Breslow 1959; Orgel 2000). Formaldehyde is formed in copious quantities in both clear and hazy low-O_2 atmospheres (Pinto et al. 1980; Pavlov and Kasting 2001). So, this may represent a more efficient way of generating glycoaldehyde than direct atmospheric chemistry. The formose reaction is not without its drawbacks, however; it would also generate a number of other sugars, which may pose problems for prebiotic synthesis (Schwartz 2007). Here, we compare production rates of glycoaldehyde from both mechanisms to see which, if either, might have provided a useful source of this important precursor molecule.

Glycolaldehyde Chemistry

Two hypothetical formation routes have been proposed to generate GA photochemically, with one route for the modern atmosphere, and one route, proposed by the authors, for conditions which may have prevailed on the early Earth. Bacher et al. (2001) suggested the following production route:

$$C_2H_4 + OH \xrightarrow{+M} HOC_2H_4^* \tag{1}$$

$$HOC_2H_4^* + O_2 \xrightarrow{+M} HOC_2H_4O_2^* \tag{2}$$

$$HOC_2H_4O_2^* + NO \longrightarrow HOC_2H_4O^* + NO_2 \tag{3}$$

$$HOC_2H_4O^* + O_2 \longrightarrow HOCH_2CHO + HO_2 \tag{4}$$

In these reactions, M represents an arbitrary unreacting third molecule that carries off excess kinetic energy. This chain of reactions, which is considered to be the dominant production route under present-day atmospheric conditions, is highly dependent on atmospheric oxygen concentrations. In the type of weakly

reducing atmosphere thought to have existed early in Earth's history (Kasting 1993; Hashimoto et al. 2007; Tian et al. 2005), a more likely chain of reactions, which has been proposed by the authors, would be:

$$C_2H_4 + OH \xrightarrow{+M} HOC_2H_4^* \tag{1}$$

$$HOC_2H_4^* + OH \xrightarrow{+M} HOCH_2CH_2OH \tag{5}$$

$$HOCH_2CH_2OH + OH \longrightarrow HOCH_2C^*HOH + H_2O \tag{6}$$

$$HOCH_2C^*HOH + OH \longrightarrow HOCH_2CHO + H_2O \tag{7}$$

Both chains begin with the hydroxyl radical adding to ethene and breaking its double bond (step 1). After that, the low-oxygen route is driven by hydroxyl interactions, whereas the Bacher et al. mechanism requires molecular oxygen at steps 2 and 4. In addition to these two routes, there is also a secondary reaction that can produce glycolaldehyde from one of the intermediate species generated in reaction 2:

$$HOC_2H_4O_2^* + HOC_2H_4O_2^* \longrightarrow HOC_2H_4OH + HOCH_2CHO + O_2 \tag{8}$$

A streamlined reaction series can be seen in Fig. 1, which contains all the reactions leading from ethene to GA. In each set of reactions, several steps lack well-constrained reaction rates, so rates from similar reactions (based on the similarity between reactants) have been used here as a proxy (see Appendix B). An analysis of estimated errors in reaction rates can be found in the Discussion. Lastly, it should be noted that the outlined formation mechanisms are not the only possible routes to producing GA, but represent the most direct synthesis from smaller molecules (a bottom-up approach). In solution, for example, metals have been proposed to catalyze the conversion of ethylene glycol ($HOCH_2CH_2OH$) to GA (Eisch et al. 2004), and photolysis of longer hydrocarbons present in either the atmosphere

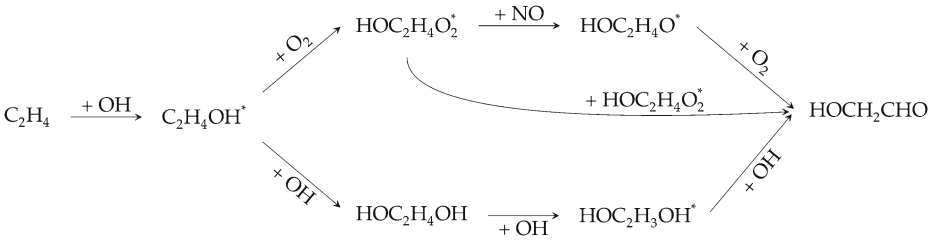

Fig. 1 Simplified series of reactions resulting in the formation of glycolaldehyde from ethene

or the surface ocean could generate GA. Aside from the consideration of the formose reaction in later sections, no aqueous reaction systems are included, and contributions from the photolysis of longer chain hydrocarbons are expected to be small.

Once GA is produced in the atmosphere, it can be transported to the surface in one of two ways: either by being incorporated into particles or by dissolving in rainwater. To simulate the first process, a new reaction was added to the photochemical model, in addition to the ones responsible for chemical production and loss. This new reaction represents the adsorption of GA onto a haze particle, based on the principles of collision theory, which we will call "sticking". With this reaction in place, the overwhelming majority of GA is drawn out of the atmosphere and sticks to the haze particles, which effectively transports the entire column production of GA to the surface ocean or any existing continental area. Second, since GA is highly soluble, with a Henrys Law coefficient of 4×10^4 M atm^{-1} (Betterton and Hoffmann 1988). This means that once GA is produced in the atmosphere, it can be transported very efficiently to the surface by rain-out, and it would be protected from photolysis while in its hydrated form (Bacher et al. 2001). Surface deposition is neglected for GA, since this contribution would be very small. These two processes individually, and in combination, control the flux of GA to the surface; the consequences of this transport will be described in further detail in the Discussion.

Model Description

We used a 1-dimensional (horizontally averaged) photochemical model to study this problem. The photochemical model is modified from the one utilized by Domagal-Goldman et al. (2011) (which was itself adapted from Kasting et al. (1979), by way of Pavlov and Kasting (2001)). It contains 88 chemical species Interacting via 443 reactions, which can be found in Appendices A and B, respectively. Table 1 contains the list of long-lived species, while Table 2 has the short-lived (intermediate) species. The mixing ratios of both CO_2 and N_2 are held constant with altitude. The model simulations shown here all have the same amount of CO_2 (5,000 ppmv, ~0.005 bar, or about 14 times the present atmospheric limit, or PAL) in a 1 bar N_2-dominated atmosphere. This amount of CO_2 was chosen as a reasonable value from a climate standpoint, based on the wide range of geological evidence and the accompanying theories (see Feulner (2012), Section 5.3 for an exhaustive review), and because of the constraints on expected abiotic methane concentrations, which will be discussed later. Methane concentrations were varied from 5 ppm to 1,500 ppm to test the system over a range of hydrocarbon haze abundance. These concentrations correspond to CH_4:CO_2 ratios from 0.001 (less than a quarter of today's ratio) to 0.3 (where polymerization of methane dominates the atmospheric chemistry). Atmospheric chemistry and transport were computed by solving a set of coupled partial differential equations, which were converted to ordinary differential equations by centered finite differencing and then integrated to steady state using the reverse Euler method. See Pavlov and Kasting (2001) for a more complete description of the model.

The model also includes UV absorption cross-sections for GA, most recently measured by Karunanandan et al. (2007), to calculate losses from photolysis. In addition, the model includes a hydrocarbon haze, along with two other types of

aerosols, S_8 and H_2SO_4. Vertical number density profiles for all three aerosols are computed using a steady-state, tridiagonal solver, which is run at each step of the time-stepping loop. The hydrocarbon haze in this model is calculated using the fractal haze properties of Wolf and Toon (2010). The key differences between spherical and fractal hazes are described by those authors. For more information about the implementation of the fractal haze algorithm, see Supplemental Materials.

Results

Figure 2 shows the total column production of both formaldehyde (H_2CO, or FA) and GA for the full range of CH_4:CO_2 ratios. As seen in Fig. 2, the strongest column-integrated production of GA occurs at a CH_4:CO_2 ratio of 0.02 (total column production for GA is $\sim 7 \times 10^5$ $cm^{-2}s^{-1}$), which is used for Figs. 3, 4 and 5. At this CH_4:CO_2 ratio, the amount of methane and hydrogen present in the atmosphere allows for a greater amount of molecular oxygen, which is integral to the Bacher et al. production route for GA. Figure 3 shows the main atmospheric gas species mixing ratios with height on the left, as well as the dominant long-chain hydrocarbons on the right. Note that the peak in hydrocarbons and water that occurs where the O_2 concentrations are reduced near 50 km. Figure 4 shows the various number densities of certain subsets of species: panel (a) shows H- and O-related radicals; panel (b) shows the various radicals produced from the photolysis of methane; panel (c) shows formaldehyde, as well as several radical precursors to species found in panel (d); and finally, panel (d) shows the immediate precursors to GA. Figure 5 has two parts: part (a) shows the vertical column production rates for several different CH_4:CO_2 ratios, and part (b) describes the dominant production and loss rates with height. Interestingly, in Fig. 5b, it can be seen that the principal production of GA is not through either route, but rather from the reaction 8. This reaction is much faster than the proposed anoxic production route and minimizes the amount of O_2 necessary to produce GA, thus offering a compromise between the anoxic and oxic production routes. The intermediate $HOC_2H_4O^*$ very rapidly decays, preventing the set of

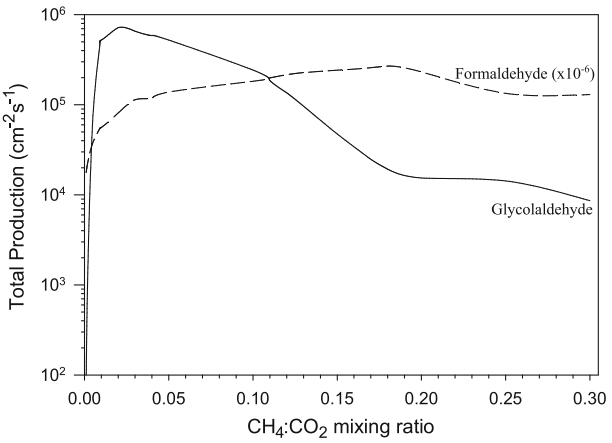

Fig. 2 Total production of both formaldehyde (*dashed line*) and glycolaldehyde (*solid line*) for a range of CH_4:CO_2 ratios. Note that the formaldehyde values are a scaled down by 10^6 (e.g., production of FA at 0.17 CH_4:CO_2 is $\sim 3 \times 10^{11}$ $cm^{-2}s^{-1}$)

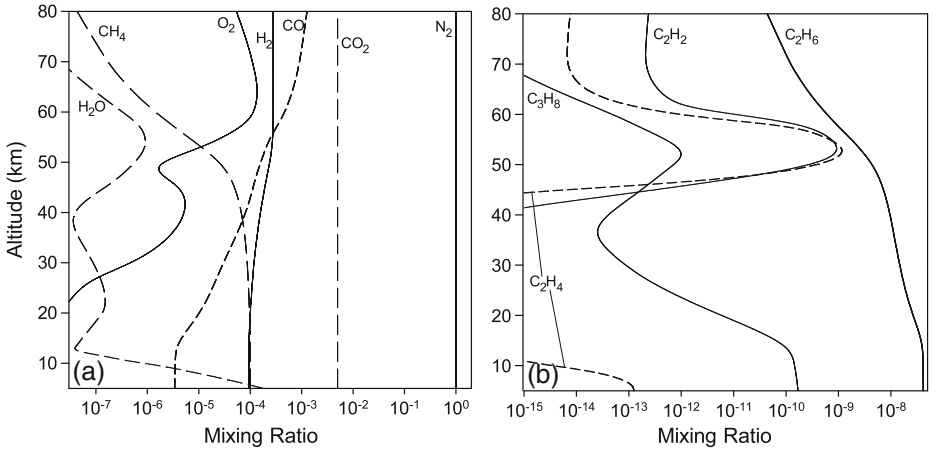

Fig. 3 Long-lived species mixing ratios (**a**), and prevalent longer-chain ordinary hydrocarbons (**b**)

reactions (reactions 1–4) proposed by Bacher et al. (2001) from going to completion. This results in the production via reaction 4 being nearly 40 orders of magnitude lower than via reaction 8.

The organic haze produced at 2 % CH_4:CO_2 is very thin (the total column optical depth at 500 nm is $\sim 7 \times 10^{-8}$), and sensitivity studies show that the haze remains thin in the visible for a much broader range of CH_4:CO_2 ratios than spherical haze under comparable conditions. The critical amount of polymerization for an optically thick haze is pushed from a CH_4:CO_2 ratio of 0.2 to closer to 0.3, due to the fractal nature of the haze. For more results regarding the haze, see the Supplemental Materials.

Discussion

Prebiotic CH_4 Concentrations

We first return to the question of how much CH_4 could have been present in the prebiotic atmosphere. Our base model assumes 100 ppmv CH_4. According to Pavlov and Kasting (2001), maintaining this atmospheric concentration would require a CH_4 source of $\sim 10^{10}$ molecules $cm^{-2}s^{-1}$, or $\sim 5 \times 10^{12}$ moles yr^{-1}, which is one-tenth of the present biological CH_4 flux (Prather 2001) (1 mole yr^{-1} = 0.00374 molecules $cm^{-2}s^{-1}$). The current abiotic flux of CH_4 from midocean ridges could be as high as 10^{12} mol yr^{-1}, based on measured CH_4 concentration of 1–2 mmol/kg at the Lost City ventfield on the Mid-Atlantic ridge (Kelley et al. 2005) and a hydrothermal circulation rate of $\sim 10^{15}$ kg/yr, estimated from heat flux measurements (Mottl and Wheat 1994). A more conservative estimate, based on the assumption that about 15 % of seafloor oxidation can be attributed to serpentinization, is that the CH_4 flux from this source is closer to 10^{11} mol yr^{-1} (Sleep 2005). This CH_4 is produced by serpentinization of peridotite, an ultramafic rock type, in the presence of dissolved CO_2 (an ultramafic rock is one that is rich in magnesium, like the mantle). This CH_4 source would need to be 5–50 times bigger on the early Earth in order to

generate 100 ppmv of atmospheric CH_4. Today, ultramafic rocks constitute only a small fraction of the oceanic crust that interacts with seawater. On the early Earth, because of its hotter mantle, much higher degrees of partial melting may have occurred during magma generation, creating thick oceanic crust that should also have been ultramafic (Moores 1986, 1993, 2002; Sleep 2007). Herzberg et al. (2010) preditcted quantitatively that Archean seafloor should have contained 18–24 % MgO, as compared to 10–13 % MgO in Phanerozoic seafloor. Thus, high prebiotic atmospheric CH_4 mixing ratios are speculative, but not implausible. If prebiotic CH_4 concentrations were lower or higher than assumed here, then atmospheric production of GA would have been lower, assuming 5,000 ppm of CO_2. The primary control on GA production in the atmosphere is the CH_4:CO_2 ratio, with a weaker dependence on the total abundance of CH_4.

Uncertainties in Atmospheric Production of Glycolaldehyde

The rates associated with reactions 1–8, with the exception of reactions 5 and 7, have well-constrained errors. Following the published rate and error data for reactions 1 and 2, the total column production varies from the reported result by less than 25 % and 20 %, respectively. The error for reaction 6 changes total column production by less than 10 %, while errors associated with reaction 8, the principal production route in the model atmosphere, vary total column production by a factor of two. Estimated errors for reaction 5 produced no significant variation in total column production, which is most likely because reaction 8 supplies the bulk of the reactant necessary for reaction 6, $HOCH_2CH_2OH$. Reaction 7 estimated errors produced only small changes ($\sim$1 %), because production via reaction 8 is the dominant formation mechanism. Reaction 4 does not play a significant role in GA production.

Perhaps the largest source of uncertainty in our model of GA production is the efficiency with which it would have been delivered to Earth's surface. We have effectively maximized this efficiency by assuming that every GA molecule that is adsorbed onto a haze particle is delivered intact to the surface. This optimistic assumption may not be correct. If instead the GA molecules reacted chemically with the compounds in the haze particles, then delivery of GA could have been much less efficient. The situation changes somewhat for GA that is produced in the troposphere (the lowest 10 km in our model). There, the haze particles would likely have acted as cloud condensation nuclei (CCN) (Engelhart et al. 2011; Twohy et al. 2005) and would have become coated with water. GA molecules that collided with these particles would have gone into solution, rather than directly attached to the surface of the haze particle, where they could become irreversibly attached to the haze particle. Some separation between the haze particle and the GA molecule greatly increases thelikelihood that GA would survive transportation through the troposphere. If we assume that only GA formed within the troposphere made it to the surface, then the rate of GA delivery would have been reduced by a factor of 2000 compared to our base model. From Fig. 2, the maximum production rate of GA is 7×10^5 cm^{-2}s^{-1}, or $\sim 2 \times 10^8$ mol yr^{-1}. So, in the troposphere-only model, this rate

would be $\sim 1 \times 10^5$ mol yr^{-1}. Below, we use the higher value for GA production; this rate is marginally able to support prebiotic synthesis.

Predicted Glycolaldehyde Concentrations in the Ocean

How low the corresponding bulk ocean GA concentration would be depends on a number of factors, such as the efficiency and mode of transport (e.g., sticking or rainout), and whether there were aqueous production routes (e.g., the formose reaction), which could have generated GA from other molecules. The latter possibility is discussed in the next section.

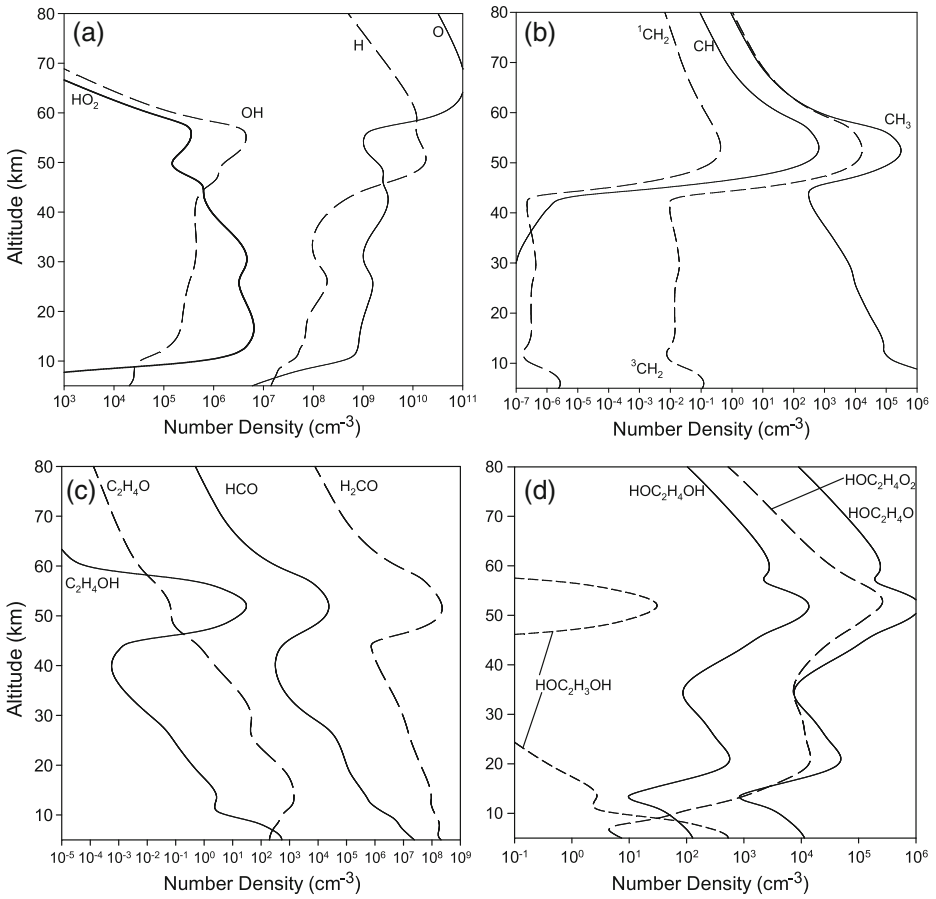

Fig. 4 Prevalent H and O radicals (**a**), methyl radicals (**b**), C_2H_4OH, C_2H_4O, and HCO radicals, alongside formaldehyde (**c**), and important GA precursor molecules (**d**)

Neglecting the formose reaction for now, we can calculate an upper limit on the dissolved GA concentration in the open ocean by balancing its production from photochemistry (from Fig. 2) with its presumed destruction when seawater passes through the midocean ridge hydrothermal vents. This neglects all other potential loss mechanisms, and thus is the most optimistic prediction for bulk ocean concentration, but a number of loss processes associated with FA (discussed in the next section) could also impact GA concentrations. As pointed out above, the maximum atmospheric production rate of GA is $\sim 2 \times 10^8$ mol yr^{-1}. At present, the time required to cycle the entire volume of the oceans (1.4×10^{21} L) through the hot axial midocean ridge hydrothermal vents is $\sim 10^7$ yr. Thus, the rate at which GA would cycle through the ridges today would be equal to its concentration times 1.4×10^{21} L/10^7 yr ($= 1.4 \times 10^{14}$ L yr^{-1}). Setting production and loss equal yields

$$C_{GA} = \frac{\text{Rate in}}{\text{Rate out}} = \frac{(\text{Rate}_{R+S+s})}{1.4 \times 10^{14}\ \text{L/yr}} = \frac{\left(2 \times 10^8\ \text{moles/yr}\right)}{1.4 \times 10^{14}\ \text{L/yr}} \approx 1 \times 10^{-6}\ \text{M} \tag{9}$$

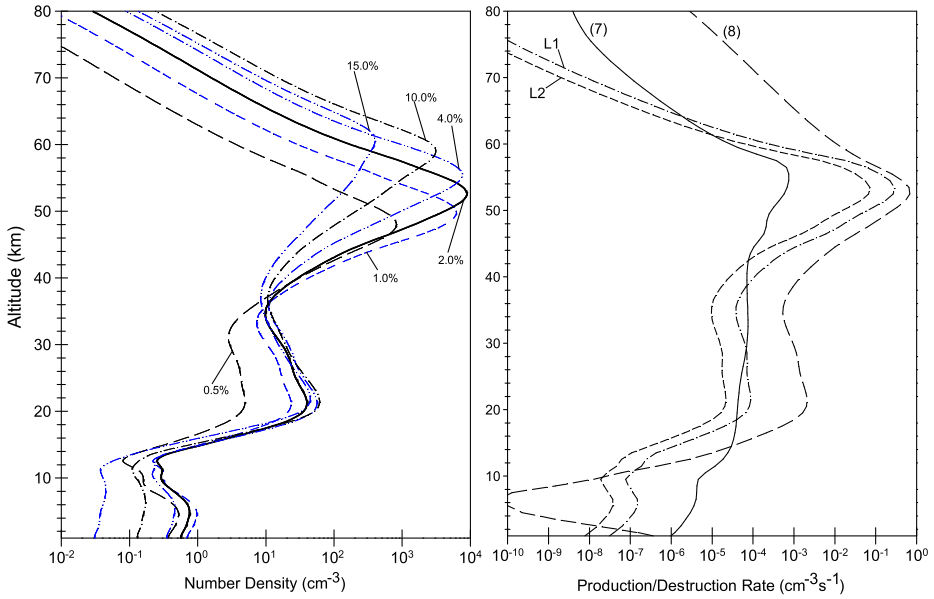

Fig. 5 Total production for GA, with varying CH_4:CO_2 ratios on the left. Note that the number densities have been reduced by a factor of a thousand. Key reactions for the production and loss of GA on the right. Reactions (7) and (8) are the production routes in the text from HOC_2H_3OH and $HOC_2H_4O_2$, respectively, while reactions L1 and L2 are destruction by OH via H-abstraction

The circulation rate through the vents may have been higher in the past (Isley 1995), and ocean volume could conceivably have been higher (Korenaga 2008), so the actual dissolved GA concentration could have been up to a factor of two or three lower or higher, respectively, even without considering other loss processes. By comparison, the concentrations of GA used in the laboratory experiments of Powner et al. (2009) were of the order of 1–2 M. So, as other authors have concluded for various other prebiotic compounds, filling the entire ocean with GA does not appear feasible, at least not by this mechanism (Schlesinger and Miller 1983). This does not necessarily indicate that the mechanism is implausible; however, it demonstrates that strong concentration processes, e.g., evaporating tide pools or eutectic freezing (Sanchez et al. 1966; Miyakawa et al. 2002), would be needed to produce GA concentrations compatible with Powner et al.'s synthesis mechanism. Regardless of the concentration mechanism, the coincident non-volatiles, such as salt, soluble metals, and more prevalent chemical species than GA, would be similarly concentrated, which may have an unanticipated effect on the concentration of GA or the synthesis mechanism outlined by Powner et al.

Production of Glycolaldehyde by Way of the Formose Reaction

A second pathway for producing GA is by way of the formose reaction (Butlerov 1861; Breslow 1959; Orgel 2000), which involves polymerization of FA into longer hydrocarbon chains. An example of the first few reactions can be seen in Fig. 6. By constrast with GA, FA should have been produced in copious quantities in the prebiotic atmosphere (Pinto et al. 1980). However, when GA production is maximized at 2 % CH_4:CO_2, FA production suffers. At 2 % CH_4:CO_2, the atmospheric production of FA is only 35 % of the production at 20 % (column-integrated production of 8.1×10^{10} versus 2.3×10^{11} [cm^{-2} s^{-1}], respectively). Neglecting the focus on the atmospheric production of GA, we will briefly consider the higher FA production levels, consistent with a CH_4:CO_2 ratio of 0.2.

For the case above, which maximizes FA production, the corresponding rate at which FA enters the oceans is 1.5×10^9 cm^{-2} s^{-1}, or $\sim 4 \times 10^{11}$ mol yr^{-1}. Following

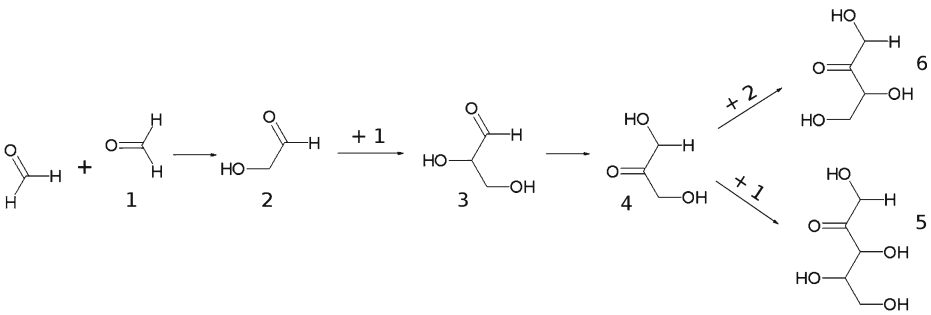

Fig. 6 The first few steps of the formose reaction

the same logic as before (i.e., assuming removal of formaldehyde at the midocean ridges), the bulk ocean concentration of FA would be 2 mM. This high concentration is an upper limit, given that there are a number of other processes, such as reactions with sulfur species, amines, HCN, and mineral surfaces, as well as the effect of varying pHs or salinities, that might control dissolved concentrations of FA (Cleaves 2008; Allou et al. 2011). Given that millimolar concentrations of FA can be sufficient to support the formose reaction (Gabel and Ponnamperuma 1967), it is possible that the hydrothermal vent system could be used to generate GA from FA. The conversion of FA into more complex organic compounds is consistent with the results of Kopetzki and Antonietti (2011), who have demonstrated that FA is removed very rapidly at the vents. In their experiments at 100 bar and a variety of temperatures (60–200 °C), a 0.5 molar concentration of formaldehyde yielded a plethora of organic molecules. Applying the experimental yields from Kopetzki and Antonietti at the much lower concentrations of FA engenders some complications. If the rate of the formose reaction is proportional to the square of the concentration of FA, it is possible that the amount of GA produced could be as much as a factor of 10^6 lower than calculated below. However, the decomposition of the longer chain products may generate GA as an intermediate, which stabilizes GA yield on longer timescales than other products; furthermore, lower concentrations may limit the degree to which polymerization occurs, which would increase the yield of GA compared to other products. Assuming, then, that the same yields remain valid for lower concentrations of FA, GA production by the hydrothermal formose reaction would result in nearly 30 μM GA, even at the lowest experimental yields (0.8 %). This level of production translates to over 2×10^9 mol yr^{-1} ($\sim 2 \times 10^8$ kg yr^{-1}), while maximum yields (1.41 %) would result in production on the order of 4×10^9 mol yr^{-1} ($\sim 3 \times 10^8$ kg yr^{-1}). This is equivalent to 20 times the maximum atmospheric production of 2×10^8 mol yr^{-1}. This suggests that, even at lower CH_4:CO_2 ratios, the formose reaction would be the dominant production pathway for GA.

Alternatives and Enhancements to the Formose Reaction

The formose reaction comes with a number of caveats and potential pitfalls. Often, the concentrations of potential reactants are less than the threshold for the autocatalytic reaction, which can limit the scope of products from the formose reaction. Additionally, the veritable zoo of products from the unmediated (i.e., without the addition of some stabilizing agent) formose reaction tend to be unstable and unsuitable for further reactions, and are most often described as a "tar". Shallow tidal pools on early continental areas have been proposed as a possible method for concentrating compounds such as GA, but given the lack of data concerning the distribution and scale of continents from the Hadean into the Archean, it is difficult to prove that such environments were widespread, or that they even existed (Korenaga 2008). Experiments on clay surfaces have been shown to be effective at removing water, which acts as another method for concentrating relevant organic compounds; Hazen and Sverjensky (2010) present a concise review of work in this direction. Stability can be aided by the addition of a mediating compound, which can limit the number of stable products, as well as increasing their longevity in solution.

The number of proposed mediating materials has grown in recent years: they include pyrite mineral surfaces (Wächtershäuser 1992), borate (Kim et al. 2011), silicates (Lambert et al. 2010), and some other metal complexes, such as molybdate, vanadate, germanate, and aluminate (Schilde et al. 1994) (see Benner et al. (2010) for a fairly comprehensive overview). Better ways of producing GA in liquid solution may exist. Pestunova et al. (2005) (as well as later experiments (Delidovich et al. 2009, 2011)) have shown that GA can be produced by UV photolysis of FA in solution. This process happens in neutral to weakly alkaline solution, so it might conceivably have occurred within the surface ocean. It might also have occurred in raindrops (because FA would have dissolved in them), but this seems less likely because the raindrops should have been acidic due to the presence of high concentrations of atmospheric CO_2.

More recently, experiments like those of Powner et al. (2009) have made progress in exploring alternatives to the formose reaction, with the introduction of phosphate into the synthesis cycle stabilizing the end product, β-ribocytidine-2',3'-cyclic phosphate. The experiments of Ritson and Sutherland (2012) have shown that derivatives of GA and GCA (glyceraldehyde) can be formed photolytically in liquid solution from HCN and H_2CO in the presence of various cyanometallates, e.g., copper cyanide complexes. This chemistry may also provide a route to assembly of pyrimidine ribonucleotides, a task that had heretofore proven difficult, though not impossible (Sanchez and Orgel 1970). If an organic haze was present, then cyanamide and cyanoacetylene could likely have been formed by reactions analogous to those that form HCN, which may have been prevalent under early Earth atmospheric conditions (Zahnle 1986; Tian et al. 2011). From there, other authors have focused on the behavior of cyanoacetylene, its potential contribution to the origins of life, and the difficulties associated with more complex prebiotic chemistry (Robertson and Miller 1995; Shapiro 1999; Nelson et al. 2000; Orgel 2002, 2004). We have not investigated such reactions explicitly, but sufficient available HCN and cyanoacetylene are two of the requirements of the mechanism proposed by Ritson and Sutherland. So, both of these routes for GA production could be promising.

Delivery of Glycolaldehyde from Space

Finally, a third method of acquiring GA is delivery from space. The organic content of meteorites is comprised principally of macromolecular organic material (Gardinier et al. 2000), while a large part of the remaining fraction would be single-carbon species, such as methane, methanol, and FA. From the molecular abundances of ices in comets, methyl formate ($HCOOCH_3$), an isomer of glycolaldehyde, represents less than a percent of the volatile composition (Ehrenfreund et al. 2002). Meteorites and comets (Chyba et al. 1990), or interplanetary dust (Anders and Grevesse 1989), could have contributed anywhere from 10^8 to 10^{10} kg yr^{-1} of organics to the early Earth. If GA represents the same fraction of organic material as its isomer methyl formate (~1 %), the amount of GA delivered from space is between 10^6 and 10^8 kg yr^{-1} ($\sim 2 \times 10^7 - 2 \times 10^9$ mol yr^{-1}). This is likely an overestimation, considering that the Murchison meteorite contains ~27 ppm of aldehydes and ketones (which includes both FA and GA) (Ehrenfreund et al. 2002), but the specific contribution of GA to the early Earth from all exogenous sources is largely unconstrained. From our

photochemical model, the production of GA directly from the atmosphere ranges from 10^7 kg yr^{-1} (best-case) to 100 kg yr^{-1} (worst-case), while production of GA from the formose reaction at the vents would be 1–2 $\times$ 10^8 kg yr^{-1}. This means that the best-case organics delivery from space would match the expected generation of GA by the formose reaction at the vents, and vent formation would dominate for more conservative values of exogenous delivery.

Conclusion

We investigated production of glycoaldehyde from three different mechanisms: (1) atmospheric photochemistry, (2) the formose reaction (in raindrops, the surface ocean, and at hydrothermal vents), and (3) delivery from space. The latter two mechanisms both can both generate a maximum of $\sim$2 $\times$ 10^8 mol yr^{-1} of GA, while mechanism (1) generates an order of magnitude less. None of these mechanisms can produce oceanic GA concentrations exceeding $\sim$2 mM. By comparison, experimental synthesis of RNA by the mechanism of Powner et al. (2009) requires 1–2 M GA. So, unless GA could somehow be greatly concentrated, by evaporation or eutectic freezing, for example, prebiotic synthesis of RNA could not have proceeded in this way.

Future research should concentrate on identifying alternative pathways for producing glycoaldehyde in the early atmosphere or oceans, or on alternative mechanisms for generating RNA, presuming than an RNA world was the first step to life as we know it. Regardless of the model assumed for the origins of life, sugars are an essential part of extant life on Earth, and represent a critical and necessary component.

Appendix A: Chemical Species

Table 1 List of long-lived chemical species

O	O_2	H_2O	H	OH	HO_2	H_2O_2
H_2	CO	HCO	H_2CO	CH_4	CH_3	C_2H_6
NO	NO_2	HNO	H_2S	HS	S	SO
HSO	SO_2	H_2SO_4	S_2	NH_3	NH_2	N_2H_4
N_2H_3	$^3CH_2$	C_2H_5	C_2H_4	C_2H_3	C_2H_2	C_3H_8
C_3H_6	C_3H_2	CH_2CCH_2	CH_3C_2H	CH_3OH	C_2H_5OH	HOC_2H_4OH
$HOC_2H_4O_2$	CH_3O_2	$C_2H_5O_2$	CH_2OH	CH_3CHO	$HOCH_2CHO$	

Table 2 List of short-lived chemical species

N	NH	HNO_2	HNO_3	$O(^1D)$	O_3
$^1SO_2$	$^3SO_2$	SO_3	S_3	NH_2^X	$CH_2^\dagger$
CH	C	C_2H	C_2	C_3H_7	C_3H_5
C_3H_3	C_2H_4OH	CH_3CO	C_2HOH	CH_3CO	C_2H_2OH
HOC_2H_4O	C_2H_5O	C_2H_4O	CH_3O	CH_3CHOH	CH_2CHOH
CH_2CO	C_2H_5CHO	HOC_2H_3OH	$HOCH_2CO$	CH_2CHO	CH_2CO
C_2H_5CHO	HOC_2H_3OH	$HOCH_2CO$	CH_2CHO	S_4	

Appendix B: Rates

Table 3 References: a, Sander et al. (2011); b, Hampson and Garvin (1977); c, Lopez et al. (2009); d, Atkinson et al. (2006); e, Aschmann and Atkinson (1998); f, Miyoshi et al. (1989); g, Orlando et al. (1998); h, Tsang (1987); i, DeMore et al. (1997); j, Tsang and Hampson (1986); k, Meier et al. (1984); l, Magneron et al. (2005); m, Cheng et al. (2002); n, Nee et al. (1985); o, Orkin et al. (2011)

Rxn. #	Reaction	Rate	Notes
325	$C_2H_4 + OH \xrightarrow{+M} C_2H_4OH$	$\begin{cases} k_0 = 1.0\times10^{-28}\times\left(\frac{300.}{T}\right)^{4.5} \\ k_\infty = 7.5\times10^{-12}\times\left(\frac{300.}{T}\right)^{0.85} \end{cases}$	updated[a]
360	$C_2H_4OH + O \longrightarrow H_2CO + CH_2OH$	$5.50\times10^{-12}\times e^{-565./T}$	As $C_2H_4 + O$[b]
361	$C_2H_4OH + OH \longrightarrow CH_2CHOH + H_2O$	$2.9\times10^{-12}\times e^{345./T}$	As $CH_3OH + OH$[a]
362	$C_2H_4OH + OH \xrightarrow{+M} HOC_2H_4OH$	$\begin{cases} k_0 = 1.0\times10^{-28}\times\left(\frac{300.}{T}\right)^{4.5} \\ k_\infty = 7.5\times10^{-12}\times\left(\frac{300.}{T}\right)^{0.85} \end{cases}$	As $C_2H_4OH + OH$[a]
363	$C_2H_4OH + HO_2 \longrightarrow C_2H_5OH + O_2$	1.7×10^{-12}	c
364	$C_2H_4OH + HO_2 \longrightarrow HOC_2H_4O + OH$	5.0×10^{-11}	c
365	$C_2H_4OH + O_2 \longrightarrow CH_2CHOH + HO_2$	9.1×10^{-12}	a
366	$HOC_2H_4O + OH \longrightarrow HOCH_2CHO + H_2O$	$2.7\times10^{-12}\times e^{20./T}$	As $C_2H_5OH + OH$[d]
367	$HOC_2H_4OH + OH \longrightarrow HOC_2H_3OH + H_2O$	1.45×10^{-11}	e
368	$HOC_2H_3OH + OH \longrightarrow HOCH_2CHO + H_2O$	$1.5\times10^{-13}\times e^{20./T}$	As $C_2H_5OH + OH$[d]
369	$C_2H_4OH + O_2 \xrightarrow{+M} HOC_2H_4O_2$	3.0×10^{-12}	f
370	$HOC_2H_4O_2 + NO \longrightarrow HOC_2H_4O + NO_2$	9.0×10^{-12}	d
371	$2\,HOC_2H_4O_2 \longrightarrow HOC_2H_4OH + HOCH_2CHO + O_2$	$3.9\times10^{-14}\times e^{1000./T}$	d
372	$2\,HOC_2H_4O_2 \longrightarrow HOC_2H_4O + HOC_2H_4O + O_2$	$3.9\times10^{-14}\times e^{1000./T}$	d
373	$HOC_2H_4O \xrightarrow{+M} H_2CO + CH_2OH$	$1.2\times10^{12}\times e^{-4750./T}\times D$	g
374	$HOC_2H_4O + O_2 \longrightarrow HOCH_2CHO + HO_2$	$6.0\times10^{-14}\times e^{-550./T}$	g
375	$HOCH_2CHO + OH \longrightarrow H_2O + HOCH_2CO$	8.8×10^{-12}	d
376	$HOCH_2CHO + OH \longrightarrow H_2O + H_2CO + HCO$	2.2×10^{-12}	modified products[d]
377	$CH_3OH + H \longrightarrow CH_3O + H_2$	$7.04\times10^{-18}\times(T^{2.1})\times e^{-2450./T}$	h
378	$CH_3OH + H \longrightarrow CH_2OH + H_2$	$2.82\times10^{-17}\times(T^{2.1})\times e^{-2450./T}$	h

Table 3 (continued)

Rxn. #	Reaction	Rate	Notes
379	$CH_3OH + CH_3O \longrightarrow CH_2OH + CH_3OH$	$5.0\times10^{-13}\times e^{-2050./T}$	h
380	$CH_3OH + OH \longrightarrow CH_2OH + H_2O$	$5.67\times10^{-18}\times(T^{2.})\times e^{140./T}$	d
381	$CH_3OH + OH \longrightarrow CH_3O + H_2O$	$1.00\times10^{-18}\times(T^{2.})\times e^{140./T}$	d
382	$CH_2OH + O \longrightarrow H_2CO + OH$	7.0×10^{-11}	h
383	$CH_2OH + O_2 \longrightarrow H_2CO + HO_2$	9.6×10^{-12}	i
384	$CH_2OH + H \longrightarrow H_2CO + H_2$	1.0×10^{-11}	h
385	$CH_2OH + H \longrightarrow CH_3 + OH$	1.6×10^{-10}	h
386	$CH_2OH + HCO \longrightarrow H_2CO + H_2CO$	3.0×10^{-10}	h
387	$CH_2OH + HCO \longrightarrow CH_3OH + CO$	2.0×10^{-10}	h
388	$CH_2OH + CH_3O \longrightarrow CH_3OH + H_2CO$	4.0×10^{-11}	h
389	$CH_2OH + CH_3 \longrightarrow CH_4 + H_2CO$	4.0×10^{-12}	h
390	$CH_2OH + OH \longrightarrow H_2CO + H_2O$	$2.9\times10^{-12}\times e^{-345./T}$	a
391	$CH_3O + H \longrightarrow H_2CO + H_2$	3.3×10^{-11}	j
392	$CH_3O + OH \longrightarrow H_2CO + H_2O$	3.0×10^{-11}	j
393	$CH_3O + HCO \longrightarrow CH_3OH + CO$	1.5×10^{-10}	j
394	$CH_3O + H_2CO \longrightarrow CH_3OH + HCO$	$1.7\times10^{-13}\times e^{-1500./T}$	j
395	$CH_3O + CO \longrightarrow CH_3 + CO_2$	$2.6\times10^{-11}\times e^{-5940./T}$	j
396	$CH_3O + CH_3OH \longrightarrow CH_2OH + CH_3OH$	$5.0\times10^{-13}\times e^{-2050./T}$	h
397	$C_2H_5OH + H \longrightarrow C_2H_5O + H_2$	$7.04\times10^{-18}\times(T^{2.1})\times e^{-2450./T}$	As $CH_3OH + H$[h]
398	$C_2H_5OH + H \longrightarrow CH_3CHOH + H_2$	$2.82\times10^{-17}\times(T^{2.1})\times e^{-2450./T}$	”
399	$C_2H_5OH + H \longrightarrow C_2H_4OH + H_2$	$2.82\times10^{-17}\times(T^{2.1})\times e^{-2450./T}$	”
400	$C_2H_5OH + OH \longrightarrow CH_3CHOH + H_2O$	$6.03\times10^{-18}\times(T^{2.})\times e^{511./T}$	d
401	$C_2H_5OH + OH \longrightarrow C_2H_4OH + H_2O$	$3.35\times10^{-19}\times(T^{2.})\times e^{511./T}$	d
402	$C_2H_5OH + OH \longrightarrow C_2H_5O + H_2O$	$3.35\times10^{-19}\times(T^{2.})\times e^{511./T}$	d
403	$CH_3 + HCO \xrightarrow{+M} CH_3CHO$	3.0×10^{-11}	j

Table 3 (continued)

Rxn. #	Reaction	Rate	Notes
404	$CH_3CO \xrightarrow{+M} CH_3 + CO$	$1.45\times10^{19}\times(T^{8.62})\times e^{-11284./T}\times D$	j
405	$CH_3CO + H \longrightarrow CH_3 + HCO$	1.6×10^{-10}	j
406	$HOCH_2CO \xrightarrow{+M} CH_2OH + CO$	$1.45\times10^{19}\times(T^{8.62})\times e^{-11284./T}\times D$	As $CH_3CO + M$[j]
407	$HOCH_2CO + H \longrightarrow CH_2OH + HCO$	1.6×10^{-10}	As $CH_3CO + H$[j]
408	$HOCH_2CO + OH \longrightarrow CH_2OH + CO + OH$	5.0×10^{-11}	As $CH_3CO + OH$[j]
409	$CH_2CHOH + H \longrightarrow C_2H_4 + OH$	1.6×10^{-10}	As $CH_2OH + H$[h]
410	$CH_2CHOH + H \longrightarrow CH_2CO + H_2$	1.0×10^{-11}	As $CH_2OH + H$[h]
411	$C_2H_5O + OH \longrightarrow C_2H_4O + H_2O$	$6.9\times10^{-12}\times e^{250./T}$	As $CH_3CHO + OH$[j]
412	$C_2H_5O + OH \longrightarrow CH_3CHO + H_2O$	$6.9\times10^{-12}\times e^{250./T}$	”
413	$C_2H_5O \xrightarrow{+M} CH_3 + H_2CO$	$1.45\times10^{19}\times(T^{8.62})\times e^{-11284./T}\times D$	As $CH_3CO + M$[j]
414	$C_2H_5O + NO \longrightarrow CH_3CHO + HNO$	1.1×10^{-11}	d
415	$CH_3O + NO \longrightarrow H_2CO + HNO$	$2.3\times10^{-12}\times(T/300.)^{-0.7}$	d
416	$C_2H_4O + OH \longrightarrow CH_3O + H_2CO$	5.0×10^{-11}	As $CH_3CO + OH$[j]
417	$C_2H_4O + H \longrightarrow H_2CO + CH_3$	1.6×10^{-10}	As $CH_3CO + H$[j]
418	$CH_2CHO + OH \longrightarrow H_2CO + H_2CO$	2.0×10^{-10}	As $CH_2OH + HCO$[h]
419	$CH_3CHOH + OH \longrightarrow CH_2CHOH + H_2O$	$8.8\times10^{-12}\times e^{-798./T}$	As $CH_3OH + OH$ [1]
420	$CH_3CHOH + OH \longrightarrow CH_3CHO + H_2O$	$2.2\times10^{-12}\times e^{-798./T}$	”
421	$CH_3CHOH + O_2 \longrightarrow CH_3CHO + HO_2$	1.9×10^{-11}	d
422	$CH_3 + O_3 \longrightarrow CH_3O + O_2$	$4.7\times10^{-12}\times e^{-210./T}$	d
423	$CH_3 + O_2 \xrightarrow{+M} CH_3O_2$	$\begin{cases} k_0 = 1.0\times10^{-30}\times\left(\frac{300.}{T}\right)^{3.3} \\ k_\infty = 1.8\times10^{-12}\times\left(\frac{300.}{T}\right)^{-1.1} \end{cases}$	d
424	$2\,CH_3O_2 \longrightarrow CH_3OH + H_2CO + O_2$	$6.49\times10^{-14}\times e^{365./T}$	d
425	$2\,CH_3O_2 \longrightarrow CH_3O + CH_3O + O_2$	$7.4\times10^{-13}\times e^{-520./T}$	d
426	$CH_3O + HCO \longrightarrow CH_3OH + CO$	1.5×10^{-10}	j
427	$CH_3O + H_2CO \longrightarrow CH_3OH + HCO$	$1.7\times10^{-13}\times e^{-1500./T}$	j
428	$C_2H_5 + O_3 \longrightarrow C_2H_5O + O_2$	$4.7\times10^{-12}\times e^{-210./T}$	As $CH_3OH + O_3$[d]

Table 3 (continued)

Rxn. #	Reaction	Rate	Notes
429	$C_2H_5 + O_2 \xrightarrow{+M} C_2H_5O_2$	$\begin{cases} k_0 = 1.0\times10^{-30}\times\left(\frac{300.}{T}\right)^{3.3} \\ k_\infty = 1.8\times10^{-12}\times\left(\frac{300.}{T}\right)^{-1.1} \end{cases}$	As $CH_3OH + O_2$[d]
430	$2\ C_2H_5O_2 \longrightarrow C_2H_5OH + C_2H_4O + O_2$	$6.49\times10^{-14}\times e^{365./T}$	As $CH_3O_2 + CH_3O_2$[d]
431	$2\ C_2H_5O_2 \longrightarrow C_2H_5O + C_2H_5O + O_2$	$7.4\times10^{-13}\times e^{-520./T}$	”
432	$C_2H_5O + HCO \longrightarrow C_2H_5OH + CO$	1.5×10^{-10}	As $CH_3CO + HCO$[j]
433	$C_2H_5O + H_2CO \longrightarrow C_2H_5OH + HCO$	$1.7\times10^{-13}\times e^{-1500./T}$	”
434	$HOCH_2CHO + h\nu \longrightarrow OH + CH_2CHO$	1.09×10^{-5}	1
435	$HOCH_2CHO + h\nu \longrightarrow CH_2OH + HCO$	8.06×10^{-5}	1
436	$HOCH_2CHO + h\nu \longrightarrow CH_3OH + CO$	1.63×10^{-5}	1
437	$HOCH_2CHO + h\nu \longrightarrow H + HOCH_2CO$	1.09×10^{-6}	1
438	$CH_3OH + h\nu \longrightarrow CH_3 + OH$	4.87×10^{-8}	cross-section from[m], reaction from[n]
439	$CH_3OH + h\nu \longrightarrow H_2CO + H_2$	1.17×10^{-6}	”
440	$CH_3OH + h\nu \longrightarrow CH_3O + H$	1.22×10^{-6}	”
441	$C_2H_5OH + h\nu \longrightarrow C_2H_5 + OH$	3.91×10^{-8}	As $CH_3OH + h\nu$, cross section from[o]
442	$C_2H_5OH + h\nu \longrightarrow C_2H_4O + H_2$	9.0×10^{-7}	”
443	$C_2H_5OH + h\nu \longrightarrow C_2H_5O + H$	2.97×10^{-6}	”
444	$HOCH_2CHO$ + aerosol $\longrightarrow$ aerosol	$R^2_{fractal}\sqrt{\frac{8\pi kT}{\mu}}$	Adsorption onto the HCAER, governed by collision theory

References

Allou L, Maimouni LE, Calvé SL (2011) Henry's law constant measurements for formaldehyde and benzaldehyde as a function of temperature and water composition. Atmos Environ 45(17):2991–2998

Anders E, Grevesse N (1989) Abundances of the elements: Meteoritic and solar. Geochim Cosmochim Acta 53(1):197–214

Aschmann S, Atkinson R (1998) Kinetics of the gas-phase reactions of the OH radical with selected glycol ethers, glycols, and alcohols. Int J Chem Kinet 30(8):533–540

Atkinson R, Baulch D, Cox R, Crowley J, Hampson R, Hynes R, Jenkin M, Rossi M, Troe J et al (2006) Evaluated kinetic and photochemical data for atmospheric chemistry: volume II: gas phase reactions of organic species. Atmos Chem Phys 6(11):3625–4055

Bacher C, Tyndall GS, Orlando JJ (2001) The atmospheric chemistry of glycolaldehyde. J Atmos Chem 39:171–189

Benner S, Kim H, Kim M, Ricardo A (2010) Planetary organic chemistry and the origins of biomolecules. Cold Spring Harbor Perspect Biol 2(7):a003467 (21 pages)

Betterton EA, Hoffmann MR (1988) Henry's Law constants of some environmentally important aldehydes. Environ Sci Technol 22:1415–1418

Breslow R (1959) On the mechanism of the formose reaction. Tetrahedron Lett 21:22–26

Butlerov A (1861) Bildung einer zuckerartigen substanz durch synthese [formation of a sugar-like substance by synthesis]. Annalen der Chemie 120:295–298

Cheng B-M, Bahou M, Lee Y-P, Lee LC (2002) Absorption cross sections and solar photodissociation rates of deuterated isotopomers of methanol. J Geophys Res 107(A8):SIA 7–1–SIA 7–5

Chyba CF, Sagan C, Brookshaw L, Thomas PJ (1989) Impact delivery of prebiotic organics to the early Earth. Orig Life Evol Biosph 19:467–468

Chyba CF, Thomas PJ, Brookshaw L, Sagan C (1990) Cometary delivery of organic molecules to the early Earth. Science 249:366–373

Cleaves HJ, Chalmers JH, Lazcano A, Miller SL, Bada JL (2008) A reassessment of prebiotic organic synthesis in neutral planetary atmospheres. Orig Life Evol Biosph 38(2):105–115

Cleaves II HJ (2008) The prebiotic geochemistry of formaldehyde. Precambrian Res 164:111–118

Delidovich I, Simonov A, Pestunova O, Parmon V (2009) Catalytic condensation of glycolaldehyde and glyceraldehyde with formaldehyde in neutral and weakly alkaline aqueous media: kinetics and mechanism. Kinet Catal 50(2):297–303

Delidovich I, Taran O, Simonov A, Matvienko L, Parmon V (2011) Photoinduced catalytic synthesis of biologically important metabolites from formaldehyde and ammonia under plausible "prebiotic" conditions. Adv Space Res 48(3):441–449

DeMore W, Sander S, Golden D, Hampson R, Kurylo M, Howard C, Ravishankara A, Kolb C, Molina M (1997) Chemical kinetics and photochemical data for use in stratospheric modeling. National Aeronautics and Space Administration, Jet Propulsion Laboratory, California Institute of Technology

Domagal-Goldman SD, Meadows VS, Claire MW, Kasting JF (2011) Using biogenic sulfur gases as remotely detectable biosignatures on anoxic planets. Astrobiology 11:419–441

Driese S, Jirsa M, Ren M, Brantley S, Sheldon N, Parker D, Schmitz M (2011) Neoarchean paleoweathering of tonalite and metabasalt: implications for reconstructions of 2.69 Ga early terrestrial ecosystems and paleoatmospheric chemistry. Precambrian Res 189(1):1–17

Ehrenfreund P, Irvine W, Becker L, Blank J, Brucato J, Colangeli L, Derenne S, Despois D, Dutrey A, Fraaije H et al (2002) Astrophysical and astrochemical insights into the origin of life. Rep Progr Phys 65(10):1427

Eisch JJ, Munson PR, Gitua JN (2004) The potential of photochemical transition metal reactions in prebiotic organic synthesis. I. observed conversion of methanol into ethylene glycol as possible prototype for sugar alcohol formation. Orig Life Evol Biosph 34(5):441–454

Emmanuel S, Ague J (2007) Implications of present-day abiogenic methane fluxes for the early Archean atmosphere. Geophys Res Lett 34(15):L15810

Engelhart GJ, Moore RH, Nenes A, Pandis SN (2011) Cloud condensation nuclei activity of isoprene secondary organic haze. JGR 116:D02207

Fegley Jr B, Schaefer L (2012) Chemistry of the Earth's earliest atmosphere. arXiv preprint arXiv:1210.0270

Feulner G (2012) The faint young Sun problem. Rev Geophys 50(2):RG2006

Gabel NW, Ponnamperuma C (1967) Model for origin of monosaccharides. Nature 216:453–455

Gaidos EJ, Güdel M, Blake GA (2000) The faint young Sun paradox: an observational test of an alternative solar model. Geophys Res Lett 27(4):501–503
Gardinier A, Derenne S, Robert F, Behar F, Largeau C, Maquet J (2000) Solid state CP/MAS ^{13}C NMR of the insoluble organic matter of the Orgueil and Murchison meteorites: quantitative study. Earth Planet Sci Lett 184(1):9–21
Hampson Jr R, Garvin D (1977) Evaluation and compilation of reaction rate data. J Phys Chem 81(25):2317–2319
Haqq-Misra JD, Domagal-Goldman SD, Kasting PJ, Kasting JF (2008) A revised, hazy methane greenhouse for the archean Earth. Astrobiology 8:1127–1136
Hashimoto GL, Abe Y, Sugita S (2007) The chemical composition of the early terrestrial atmosphere: formation of a reducing atmosphere from CI-like material. JGR 112:E05010
Hazen R, Sverjensky D (2010) Mineral surfaces, geochemical complexities, and the origins of life. Cold Spring Harbor Perspect Biol 2(5):a002162 (21 pages)
Herzberg C, Condie K, Korenaga J (2010) Thermal history of the Earth and its petrological expression. Earth Planet Sci Lett 292(1):79–88
Isley AE (1995) Hydrothermal plumes and the delivery of iron to banded iron formation. J Geology 103(2):169–185
Karunanandan R, Hölsher D, Dillon TJ, Horowitz A, Crowley JN (2007) Reaction of OH with glycolaldehyde, $HOCH_2CHO$: rate coefficients (240-362 K) and mechanism. J Phys Chem 111:897–908
Kasting JF (1993) Earth's early atmosphere. Science 259:920–926
Kasting JF, Liu SC, Donahue TM (1979) Oxygen levels in the prebiological atmosphere. J Geophys Res 84:3097–3107
Kelley DS, Karson JA, Früh-Green G, Yoerger D, Shank T, Butterfield D, Hayes J, Schrenk M, Olson E, Proskurowski G et al (2005) A serpentinite-hosted ecosystem: the Lost City hydrothermal field. Science 307(5714):1428–1434
Kharecha P, Kasting J, Siefert J (2005) A coupled atmosphere-ecosystem model of the early archean earth. Geobiology 3(2):53–76
Kim H, Ricardo A, Illangkoon H, Kim M, Carrigan M, Frye F, Benner S (2011) Synthesis of carbohydrates in mineral-guided prebiotic cycles. J Am Chem Soc 133(24):9457–9468
Kopetzki D, Antonietti M (2011) Hydrothermal formose reaction. New J Chem 35:1787–1794
Korenaga J (2008) Plate tectonics, flood basalts and the evolution of Earth's oceans. Terra Nova 20:419–439
Lambert J, Gurusamy-Thangavelu S, Ma K (2010) The silicate-mediated formose reaction: bottom-up synthesis of sugar silicates. Science 327(5968):984–986
Lazar C, McCollom T, Manning C (2012) Abiogenic methanogenesis during experimental komatiite serpentinization: implications for the evolution of the early Precambrian atmosphere. Chem Geol 326-327:102–112
Lopez J, Rasmussen C, Alzueta M, Gao Y, Marshall P, Glarborg P (2009) Experimental and kinetic modeling study of C_2H_4 oxidation at high pressure. Proc Combust Inst 32(1):367–375
Magneron I, Mellouki A, Bras GL, Moortgat GK, Horowitz A, Wirtz K (2005) Photolysis and OH-initiated oxidation of glycolaldehyde under atmospheric conditions. J Phys Chem 109:4552–4561
Maurette M, Duprat J, Engrand C, Gounelle M, Kurat G, Matrajt G, Toppani A (2000) Accretion of neon, organics, CO_2, nitrogen and water from large interplanetary dust particles on the early Earth. Planet Space Sci 48:1117–1137
Meier U, Grotheer H, Just T (1984) Temperature dependence and branching ratio of the CH_3OH + OH reaction. Chem Phys Lett 106(1):97–101
Menor-Salván C, Ruiz-Bermejo D, Guzmán MI, Osuna-Esteban S, Veintemillas-Verdaguer S (2009) Synthesis of pyrimidines and triazines in ice: implications for the prebiotic chemistry of nucleobases. Chem Eur J 15(17):4411–4418
Miller SL (1953) A production of amino acids under possible primitive Earth conditions. Science 117:528–529
Miyakawa S, Cleaves HJ, Miller SL (2002) The cold origin of life: B. Implications based on pyrimidines and purines produced from frozen ammonium cyanide solutions. Orig Life Evol Biosph 32(3):209–218
Miyoshi A, Matsui H, Washida N (1989) Reactions of hydroxyethyl radicals with oxygen and nitric oxide. Chem Phys Lett 160(3):291–294
Moores EM (1986) The proterozoic ophiolite problem, continental emergence, and the Venus connection. Science 234(4772):65

Moores EM (1993) Neoproterozoic oceanic crustal thinning, emergence of continents, and origin of the phanerozoic ecosystem: a model. Geology 21(1):5–8
Moores EM (2002) Pre-1 Ga (pre-Rodinian) ophiolites: their tectonic and environmental implications. Geol Soc Amer Bull 114(1):80–95
Mottl MJ, Wheat CG (1994) Hydrothermal circulation through mid-ocean ridge flanks: fluxes of heat and magnesium. Geochim Cosmochim Acta 58(10):2225–2237
Nee J, Suto M, Lee L (1985) Photoexcitation processes of CH_3OH: Rydberg states and photofragment fluorescence. Chem Phys 98(1):147–155
Nelson KE, Levy M, Miller SL (2000) Peptide nucleic acids rather than RNA may have been the first genetic molecule. Proc Natl Acad Sci 97(8):3868–3871
Orgel LE (2000) Self-organizing biochemical cycles. Proc Natl Acad Sci, USA 97(23):12503–12507
Orgel LE (2002) Is cyanoacetylene prebiotic? Orig Life Evol Biosph 32(3):279–281
Orgel LE (2004) Prebiotic adenine revisited: eutectics and photochemistry. Orig Life Evol Biosph 34(4):361–369
Orkin VL, Khamaganov VG, Martynova LE, Kurylo MJ (2011) High-accuracy measurements of OH· reaction rate constants and IR and UV absorption spectra: ethanol and partially fluorinated ethyl alcohols. J Phys Chem A 115(31):8656–8668
Orlando JJ, Tyndall GS, Bilde M, Ferronato C, Wallington TJ, Vereecken L, Peeters J (1998) Laboratory and theoretical study of the oxy radicals in the OH- and Cl-initiated oxidation of ethene. J Phys Chem A 102(42):8116–8123
Pavlov AA, Kasting JF (2001) UV shielding of NH_3 and O_2 by organic hazes in the Archean atmosphere. J Geophys Res 106:23267–23287
Pestunova O, Simonov A, Snytnikov V, Stoyanovsky V, Parmon V (2005) Putative mechanism of the sugar formation on prebiotic Earth initiated by UV-radiation. Adv Space Res 36(2):214–219
Pinto JP, Gladstone GR, Yung YL (1980) Photochemical production of formaldehyde in Earth's primitive atmosphere. Science 210:183–185
Powner MW, Gerland B, Sutherland JD (2009) Synthesis of activated pyrimidine ribonucleotides in prebiotically plausible conditions. Nature 459:239–242
Prather M (2001) Atmospheric chemistry and greenhouse gases. In: Houghton J, Ding Y, Griggs D, Noguer M, van der Linden P, Dai X, Maskell K, Johnson C (eds) Climate change 2001: the scientific basis, vol 881. Cambridge University Press, Cambridge, pp 239–288
Ritson D, Sutherland J (2012) Prebiotic synthesis of simple sugars by photoredox systems chemistry. Nature Chem 4:895–899
Robertson MP, Miller SL (1995) An efficient prebiotic synthesis of cytosine and uracil. Nature 375:772–774
Rosing MT, Bird DK, Sleep NH, Bjerrum CJ (2010) No climate paradox under the faint early sun. Nature 464(7289):744–747
Sagan C, Chyba C (1997) The early faint young Sun paradox: organic shielding of ultraviolet-labile greenhouse gases. Science 276:1217–1221
Sanchez R, Ferris J, Orgel L (1966) Conditions for purine synthesis: did prebiotic synthesis occur at low temperatures? Science 153(3731):72–73
Sanchez RA, Orgel LE (1970) Studies in prebiotic synthesis: V. synthesis and photoanomerization of pyrimidine nucleosides. J Mol Biol 47(3):531–543
Sander SP, Abbatt J, Barker JR, Burkholder JB, Friedl RR, Golden DM, Huie RE, Kolb CE, Kurylo MJ, Moortgat GK, Orkin VL, Wine PH (2011) Chemical kinetics and photochemical data for use in atmospheric studies, evaluation no. 17. JPL Publication 10-6, Jet Propulsion Laboratory, Pasadena. http://jpldataeval.jpl.nasa.gov
Schilde U, Kraudelt H, Uhlemann E (1994) Separation of the oxoanions of germanium, tin, arsenic, antimony, tellurium, molybdenum and tungsten with a special chelating resin containing methylaminoglucitol groups. React Polym 22(2):101–106
Schlesinger G, Miller SL (1983) Prebiotic synthesis in atmospheres containing CH_4, CO, and CO_2. J Mol Evol 19(5):383–390
Schwartz AW (2007) Intractable mixtures and the origin of life. Chem Biodivers 4(4):656–664
Shapiro R (1984) The improbability of prebiotic nucleic acid synthesis. Orig life 14(1–4):565–570
Shapiro R (1988) Prebiotic ribose synthesis: a critical analysis. Orig Life Evol Biosph 18(1–2):71–85
Shapiro R (1999) Prebiotic cytosine synthesis: a critical analysis and implications for the origin of life. Proc Natl Acad Sci 96(8):4396–4401
Sleep NH (2005) Dioxygen over geologic time. Met Ions Biol Syst 43:49–73

Sleep NH (2007) Plate tectonics through time. In: Treatise on geophysics, pp 145–169
Sleep NH, Zahnle K (2001) Carbon dioxide cycling and implications for climate on ancient earth. J Geoph Res 106:1373–1400
Szostak JW (2009) Systems chemistry on early earth. Nature 459:171–172
Tian F, Kasting JF, Zahnle K (2011) Revisiting HCN formation in Earth's early atmosphere. Earth Planet Sci Lett 308:417–423
Tian F, Toon OB, Pavlov AA, Sterck HD (2005) A hydrogen-rich early Earth atmosphere. Science 308:1014–1017
Trainer MG, Pavlov AA, Dewitt HL, Jimenez JL, McKay CP, Toon OB, Tolbert MA (2006) Organic haze on Titan and the early Earth. Proc Natl Acad Sci 103:18035–18042
Tsang W (1987) Chemical kinetic data base for combustion chemistry. Part 2. Methanol. J Phys Chem Ref Data 16(3):471–508
Tsang W, Hampson R (1986) Chemical kinetic data base for combustion chemistry. Part I. Methane and related compounds. J Phys Chem Ref Data; (United States) 15(3):1087 (193 pages)
Twohy CH, Anderson JR, Crozier PA (2005) Nitrogenated organic aerosols as cloud condensation nuclei. Geoph Res Letters 32:L19805
Ueno Y, Johnson MS, Danielache SO, Eskebjerg C, Pandey A, Yoshida N (2009) Geological sulfur isotopes indicate elevated OCS in the Archean atmosphere, solving faint young Sun paradox. Proc Natl Acad Sci 106(35):14784–14789
Wächtershäuser G (1992) Groundworks for an evolutionary biochemistry: the iron-sulphur world. Prog Biophys Mol Bio 58(2):85
Walker JCG (1985) Carbon dioxide on the early Earth. Orig Life 16:117–127
Wolf ET, Toon OB (2010) Fractal organic hazes provided an ultraviolet shield for early earth. Science 328:1266–1268
Zahnle KJ (1986) Photochemistry of methane and the formation of hydrocyanic acid (HCN) in the Earth's early atmosphere. J Geophys Res 91:2819–2834